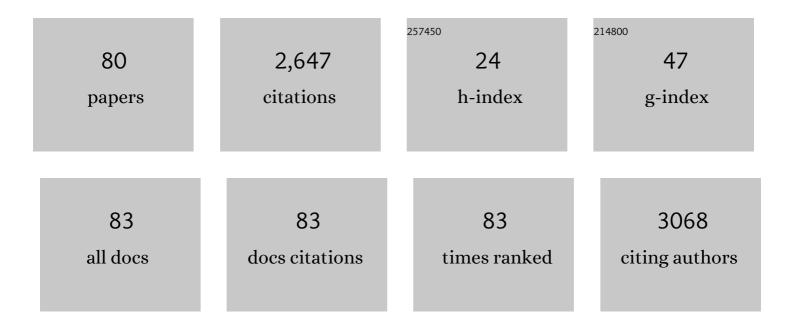
Xiaofeng Zhang

List of Publications by Year in descending order

Source: https://exaly.com/author-pdf/894392/publications.pdf Version: 2024-02-01



#	Article	IF	CITATIONS
1	Genome sequence and genetic diversity of the common carp, Cyprinus carpio. Nature Genetics, 2014, 46, 1212-1219.	21.4	576
2	An Atomic Structure of the Human Spliceosome. Cell, 2017, 169, 918-929.e14.	28.9	215
3	Structure of the human activated spliceosome in three conformational states. Cell Research, 2018, 28, 307-322.	12.0	163
4	Structure of a human catalytic step I spliceosome. Science, 2018, 359, 537-545.	12.6	118
5	HCK is a survival determinant transactivated by mutated MYD88, and a direct target of ibrutinib. Blood, 2016, 127, 3237-3252.	1.4	93
6	The cryo-EM structure of the SF3b spliceosome complex bound to a splicing modulator reveals a pre-mRNA substrate competitive mechanism of action. Genes and Development, 2018, 32, 309-320.	5.9	89
7	Structures of the human pre-catalytic spliceosome and its precursor spliceosome. Cell Research, 2018, 28, 1129-1140.	12.0	85
8	Structures of the human spliceosomes before and after release of the ligated exon. Cell Research, 2019, 29, 274-285.	12.0	74
9	A Consensus Linkage Map Provides Insights on Genome Character and Evolution in Common Carp (Cyprinus carpio L.). Marine Biotechnology, 2013, 15, 275-312.	2.4	67
10	A pot-economical and diastereoselective synthesis involving catalyst-free click reaction for fused-triazolobenzodiazepines. Green Chemistry, 2016, 18, 2642-2646.	9.0	52
11	A robot finger joint driven by hybrid multi-DOF piezoelectric ultrasonic motor. Sensors and Actuators A: Physical, 2011, 169, 206-210.	4.1	49
12	Gonadal transcriptomic analysis of yellow catfish (Pelteobagrus fulvidraco): identification of sex-related genes and genetic markers. Physiological Genomics, 2014, 46, 798-807.	2.3	46
13	Acoustic Radiation Force of a Gaussian Beam Incident on Spherical Particles in Water. Ultrasound in Medicine and Biology, 2012, 38, 2007-2017.	1.5	39
14	Organocatalytic One-Pot Asymmetric Synthesis of Thiolated Spiro-Î ³ -lactam Oxindoles Bearing Three Stereocenters. Journal of Organic Chemistry, 2016, 81, 5362-5369.	3.2	39
15	Improved clustering algorithms for image segmentation based on non-local information and back projection. Information Sciences, 2021, 550, 129-144.	6.9	39
16	Recyclable Organocatalystâ€Promoted Oneâ€Pot Asymmetric Synthesis of Spirooxindoles Bearing Multiple Stereogenic Centers. Advanced Synthesis and Catalysis, 2015, 357, 3820-3824.	4.3	38
17	One-pot and catalyst-free synthesis of pyrroloquinolinediones and quinolinedicarboxylates. Green Chemistry, 2017, 19, 3851-3855.	9.0	37
18	Cascade Knoevenagel and aza-Wittig reactions for the synthesis of substituted quinolines and quinolin-4-ols. Green Chemistry, 2019, 21, 349-354.	9.0	37

#	Article	IF	CITATIONS
19	One-Pot Synthesis of Polycyclic Spirooxindoles via Montmorillonite K10-Catalyzed C–H Functionalization of Cyclic Amines. ACS Sustainable Chemistry and Engineering, 2018, 6, 5574-5579.	6.7	36
20	Al2O3-modified PS-PVD 7YSZ thermal barrier coatings for advanced gas-turbine engines. Npj Materials Degradation, 2020, 4, .	5.8	31
21	Sequential (3 + 2) cycloaddition and (5 + <i>n</i>) annulation for modular synthesis of dihydrobenzoxazines, tetrahydrobenzoxazepines and tetrahydrobenzoxazocines. Green Chemistry, 2018, 20, 3134-3139.	9.0	30
22	TFPI is a colonic crypt receptor for TcdB from hypervirulent clade 2 C.Âdifficile. Cell, 2022, 185, 980-994.e15.	28.9	30
23	Multilevel Image Thresholding Using Tsallis Entropy and Cooperative Pigeon-inspired Optimization Bionic Algorithm. Journal of Bionic Engineering, 2019, 16, 954-964.	5.0	28
24	Finite series expansion of a Gaussian beam for the acoustic radiation force calculation of cylindrical particles in water. Journal of the Acoustical Society of America, 2015, 137, 1826-1833.	1.1	27
25	Quantitative trait loci (QTL) associated with growth rate trait in common carp (Cyprinus carpio). Aquaculture International, 2013, 21, 1373-1379.	2.2	25
26	Acoustic radiation force on a fluid cylindrical particle immersed in water near an impedance boundary. Journal of the Acoustical Society of America, 2017, 141, 4633-4641.	1.1	25
27	One-Pot Double [3 + 2] Cycloadditions for Diastereoselective Synthesis of Pyrrolidine-Based Polycyclic Systems. Journal of Organic Chemistry, 2018, 83, 13536-13542.	3.2	24
28	One-pot synthesis of tetrahydro-pyrrolobenzodiazepines and tetrahydro-pyrrolobenzodiazepinones through sequential 1,3-dipolar cycloaddition/ <i>N</i> -alkylation (<i>N</i> -acylation)/Staudinger/aza-Wittig reactions. Green Chemistry, 2019, 21, 4489-4494.	9.0	24
29	Double 1,3-Dipolar Cycloadditions of Two Nonstabilized Azomethine Ylides for Polycyclic Pyrrolidines. Organic Letters, 2019, 21, 2176-2179.	4.6	21
30	Phononic-Crystal-Enabled Dynamic Manipulation of Microparticles and Cells in an Acoustofluidic Channel. Physical Review Applied, 2020, 13, .	3.8	21
31	Optimization and Parameters Estimation in Ultrasonic Echo Problems Using Modified Artificial Bee Colony Algorithm. Journal of Bionic Engineering, 2015, 12, 160-169.	5.0	20
32	Sequential decarboxylative [3+2] cycloaddition and Staudinger/aza-Wittig reactions for diastereoselective synthesis of tetrahydro-pyrroloquinazolines and tetrahedro-pyrrolobenzodiazepines. Tetrahedron Letters, 2020, 61, 151392.	1.4	19
33	Synthesis of tetrahydropyrrolothiazoles through one-pot and four-component N,S-acetalation and decarboxylative [3+2] cycloaddition. Green Synthesis and Catalysis, 2021, 2, 74-77.	6.8	19
34	Lysine Demethylase 5A Is Required for MYC-Driven Transcription in Multiple Myeloma. Blood Cancer Discovery, 2021, 2, 370-387.	5.0	19
35	Diffusion interface layer controlling the acceptor phase of bilayer near-infrared polymer phototransistors with ultrahigh photosensitivity. Nature Communications, 2022, 13, 1332.	12.8	19
36	PASE synthesis of pyrrolidine-containing heterocycles through [3+2] cycloaddition-initiated reactions. Current Opinion in Green and Sustainable Chemistry, 2018, 11, 65-69.	5.9	18

#	Article	IF	CITATIONS
37	Study on tangentially polarized composite cylindrical piezoelectric transducer with high electro-mechanical coupling coefficient. Ultrasonics, 2017, 74, 204-210.	3.9	17
38	Phase permutation entropy: A complexity measure for nonlinear time series incorporating phase information. Physica A: Statistical Mechanics and Its Applications, 2021, 568, 125686.	2.6	17
39	Recyclable organocatalyst-promoted one-pot Michael/aza-Henry/lactamization reactions for fluorinated 2-piperidinones bearing four stereogenic centres. RSC Advances, 2015, 5, 71071-71075.	3.6	16
40	Inhibition of Polo-like kinase 1 (PLK1) facilitates the elimination of HIV-1 viral reservoirs in CD4 ⁺ T cells ex vivo. Science Advances, 2020, 6, eaba1941.	10.3	16
41	Dynamical complexity changes during two forms of meditation. Physica A: Statistical Mechanics and Its Applications, 2011, 390, 2381-2387.	2.6	15
42	One-pot synthesis of dihydroquinazolinethione-based polycyclic system. Tetrahedron Letters, 2018, 59, 3845-3847.	1.4	14
43	Computation of the Acoustic Radiation Force on a Rigid Cylinder in Off-Axial Gaussian Beam Using the Translational Addition Theorem. Acta Acustica United With Acustica, 2016, 102, 334-340.	0.8	13
44	[3+2] Cycloaddition-based one-pot synthesis of 3,9-diazabicyclo[4.2.1]nonane-containing scaffold. Chemistry of Heterocyclic Compounds, 2017, 53, 468-473.	1.2	13
45	A method to depress the transmitting voltage response fluctuation of a double excitation piezoelectric transducer. Applied Acoustics, 2020, 158, 107066.	3.3	13
46	Atomically dispersed Co atoms in nitrogen-doped carbon aerogel for efficient and durable oxygen reduction reaction. International Journal of Hydrogen Energy, 2021, 46, 36836-36847.	7.1	13
47	Studies on quantitative trait loci related to superoxide dismutase in mirror carp (<i>Cyprinus) Tj ETQq1 1 0.7843</i>	814 rgBT /0 1.8	Overlock 10 T
48	Axial acoustic radiation force on a rigid cylinder near an impedance boundary for on-axis Gaussian beam. Wave Motion, 2017, 74, 182-190.	2.0	12
49	Synthesis of trifluoromethylated pyrrolidines via decarboxylative [3+2] cycloaddition of non-stabilized N -unsubstituted azomethine ylides. Journal of Fluorine Chemistry, 2017, 204, 18-22.	1.7	11
50	Acoustic radiation force of a solid elastic sphere immersed in a cylindrical cavity filled with ideal fluid. Wave Motion, 2018, 80, 37-46.	2.0	11
51	Acoustic radiation force on a rigid cylinder in an off-axis Gaussian beam near an impedance boundary. Wave Motion, 2018, 83, 111-120.	2.0	11
52	Recyclable Organocatalyst for Oneâ€Pot Asymmetric Synthesis of Dihydrofuranone and Tetrahydropyranone Spirooxindoles. European Journal of Organic Chemistry, 2019, 2019, 150-155.	2.4	11
53	Patch-based fuzzy clustering for image segmentation. Soft Computing, 2019, 23, 3081-3093.	3.6	11
54	Structure of the yeast Swi/Snf complex in a nucleosome free state. Nature Communications, 2020, 11, 3398.	12.8	11

4

#	Article	IF	CITATIONS
55	Genetic mapping and QTL analysis for body weight in Jian carp (Cyprinus carpio var. Jian) compared with mirror carp (Cyprinus carpio L.). Chinese Journal of Oceanology and Limnology, 2015, 33, 636-649.	0.7	10
56	Rear Earth Oxide Multilayer Deposited by Plasma Spray-Physical Vapor Deposition for Envisaged Application as Thermal/Environmental Barrier Coating. Coatings, 2021, 11, 889.	2.6	10
57	Synthesis of pyrrolidinedione-fused hexahydropyrrolo[2,1- <i>a</i>]isoquinolines via three-component [3 + 2] cycloaddition followed by one-pot <i>N</i> -allylation and intramolecular Heck reactions. Beilstein Journal of Organic Chemistry, 2020, 16, 1225-1233.	2.2	9
58	Study on acoustic radiation force of an elastic sphere in an off-axial Gaussian beam using localized approximation. Journal of the Acoustical Society of America, 2022, 151, 2602-2612.	1.1	9
59	Microstructural and columnar growth characteristics of 7YSZ thermal barrier coatings fabricated by plasma spray physical vapor deposition. Journal of the European Ceramic Society, 2021, 41, 315-323.	5.7	8
60	Cadmium regulates FKBP5 through miR-9-5p and induces carp lymphocyte apoptosis. Fish and Shellfish Immunology, 2022, 120, 353-359.	3.6	8
61	Thermal shock resistance of thermal barrier coatings modified by selective laser remelting and alloying techniques. Journal of the American Ceramic Society, 2022, 105, 6345-6358.	3.8	8
62	Three-component [3 + 2] cycloaddition for regio- and diastereoselective synthesis of spirooxindole-pyrrolidines. New Journal of Chemistry, 0, , .	2.8	7
63	A novel underwater image restoration method based on decomposition network and physical imaging model. International Journal of Intelligent Systems, 2022, 37, 5672-5690.	5.7	7
64	One-pot diastereoselective synthesis of tetrahydroepimino-benzo[b]azocines through sequential [3+2]-cycloaddition and Staudinger-aza-Wittig reactions. Tetrahedron Letters, 2019, 60, 151127.	1.4	6
65	PU.1 affects proliferation of the human acute myeloid leukemia U937 cell line by directly regulating MEIS1. Oncology Letters, 2015, 10, 1912-1918.	1.8	5
66	Axial acoustic radiation force on a spherical particle in a zero-order Mathieu beam. Journal of the Acoustical Society of America, 2019, 145, 3233-3241.	1.1	5
67	A low-frequency longitudinal vibration transducer with a helical slot structure. Journal of the Acoustical Society of America, 2019, 145, 2948-2954.	1.1	4
68	Analysis of acoustic radiation force on a rigid sphere in a fluid-filled cylindrical cavity with an abruptly changed cross-section. Journal of the Acoustical Society of America, 2020, 147, 516-524.	1.1	4
69	A modified fuzzy clustering algorithm based on dynamic relatedness model for image segmentation. Visual Computer, 0, , 1.	3.5	4
70	Coded Permutation Entropy: A Measure for Dynamical Changes Based on the Secondary Partitioning of Amplitude Information. Entropy, 2020, 22, 187.	2.2	2
71	Elite allele mining for growth rate traits in common carp (Cyprinus carpio) by association analysis. Aquaculture Research, 2021, 52, 1192-1200.	1.8	2
72	The acoustic radiation force on a multi-layered polymer capsule placed in a fluid-filled tube. Ultrasonics, 2021, 113, 106365.	3.9	2

#	Article	IF	CITATIONS
73	One-pot, two-step synthesis of 3,4-dihydroquinazoline-2(1H)-thiones from o-azidobenzenealdehydes, aryl amines and carbon disulfide. Tetrahedron Letters, 2021, 81, 153361.	1.4	2
74	Generalized phase permutation entropy algorithm based on two-index entropy. Scientia Sinica Informationis, 2019, 49, 1205-1216.	0.4	2
75	A High-Density Genetic Linkage Map and Fine Mapping of QTL For Feed Conversion Efficiency in Common Carp (Cyprinus carpio). Frontiers in Genetics, 2021, 12, 778487.	2.3	2
76	Exploring the underlying mechanism of acoustic radiation force on a sphere in a fluid-filled rigid tube. AIP Advances, 2021, 11, 075228.	1.3	1
77	In Situ High-Temperature Tensile Fracture Mechanism of PS-PVD EBCs. Coatings, 2022, 12, 655.	2.6	1
78	Three-dimensional acoustic radiation force of a sphere arbitrarily positioned in a Gaussian beam. Proceedings of Meetings on Acoustics, 2019, , .	0.3	0
79	A radial vibration low frequency transducer with periodic axial slotted structure. Proceedings of Meetings on Acoustics, 2019, , .	0.3	0
80	Acoustic radiation force on a rigid microsphere in a fluid-filled rigid cylindrical cavity with Helmholtz resonator end. Proceedings of Meetings on Acoustics, 2019, , .	0.3	0